SLAC–PUB–6337
SLAC/SSRL–0052
LBL–34542
August 1993
(I/SSRL-M)

The Adjustable Phase Planar Helical Undulator*

Roger Carr

Stanford Linear Accelerator Center
Stanford Synchrotron Radiation Laboratory
Stanford University
Stanford, CA 94309 USA

Steve Lidia

Advanced Light Source and Center for Beam Physics
Lawrence Berkeley Laboratory
Berkeley, California 94720

ABSTRACT

The study of magnetic and biological materials which exhibit magnetic circular dichroism has created a demand for circularly polarized x-rays whose helicity may be switched between the right and left hand senses. At present, circularly polarized x-rays are obtained from storage ring bending magnets by accepting radiation from above and below the axis, but insertion device sources are desired for greater intensity. Planar helical undulators are magnetic insertion devices that generate helical magnetic fields. The charged particle beam executes a helical trajectory in the device, and produces elliptically polarized x-rays. The special case of circularly polarized x-rays is most in demand.

We present here the design description of a new type of planar helical undulator, which we are constructing for the SPEAR storage ring at the Stanford Synchrotron Radiation Laboratory (SSRL). It comprises four rows of pure permanent magnet blocks, one row in each quadrant about the axis defined by the electron beam. Rows may be translated longitudinally with respect to each other to change the helicity of the magnetic field they create at the position of the beam. They may also be translated longitudinally to vary the energy of the x-rays emitted, unlike designs where this function is performed by varying the gap between the rows. This work includes numerical calculations of the fields, electron trajectories, x-ray spectra, off-axis effects, and mechanical design considerations.

1. INTRODUCTION

Because of a rising demand from the SSRL user community, we propose to install an insertion device on the SPEAR storage ring to produce elliptically polarized soft x-rays. The experiments driving this project involve magnetic and biological circular dichroic effects in the first row transition elements whose x-ray absorption edges fall between 550 and 950 eV. Especially important are studies of magnetic-nonmagnetic multilayers which offer promise as magnetic storage media. We propose to place an elliptically polarizing undulator (EPU) on the SPEAR beamline 5 multi-undulator mover. Beamline 5 is equipped with a grating monochromator and optics optimized for the 10-1200 eV photon energy range, and in particular, with a 2^{o} grating suitable for the entire 550-950 eV range. We have adopted the planar helical undulator concept as most practical for our needs, and have chosen a magnet design which is a variant of Sasaki's.[1,2] In this paper, the design will be described in detail. We chose our design based on an earlier general review of planar helical undulator concepts.[3]

Since we propose to place the EPU on the beamline 5 undulator mover, it is appropriate to describe that device and the insertion region where the new undulator will be installed. Further description may be found in reference 4. The beamline 5

* Work supported by Department of Energy contracts DE–AC03–76SF00515 (SLAC) and DE–AC03–76SF00098 (LBL).

Presented at the SPIE's 1993 International Symposium on Optics, Imaging and Instrumentation San Diego, CA, July 11–16, 1993

undulator mover allows one of five jaw pairs to be positioned over the electron beampipe. It moves the pairs in the horizontal transverse direction, and is also capable of adjusting the gap between the jaws from 30 mm to 300 mm. The maximum length available for insertion devices is 185 cm. At both ends of the insertion region, there are dipole trim compensation 'C' magnets which are driven by SPEAR control. In current practice, about 100 mA is injected into SPEAR, and the electron energy is 3.0 GeV. The present SPEAR beam parameters in the insertion region are shown in table 1: [5]

βx = 16.4 m	ε_x = 129 nm-rad	σ_x = 1.64 mm	σ_x' = 89 μrad
βy = 1.9 m	ε_y = 3 nm-rad	σ_y = .07 mm	σ_y' = 40 μrad

Table 1: Beta function, emittance, beam diameter and divergence for the horizontal (x) and vertical (y) directions.

2. MAGNET ARRAY DESIGN

One period of the EPU magnet arrangement is shown schematically in figure 1. There are four rows of magnets, two in each jaw. Each row is a standard Halbach sinusoidal array of pure permanent magnet material with no permeable materials.[6] The electron beam enters along the z-axis, and for Δ between 0 and $\pm \lambda/2$ it feels a helical magnetic field, and executes a helical trajectory. The resulting acceleration causes the emission of elliptically polarized x-rays. If $\Delta = 0$, the x-rays are linearly polarized vertically, and if $\Delta = \pm \lambda/2$, the x-rays are linearly polarized horizontally.

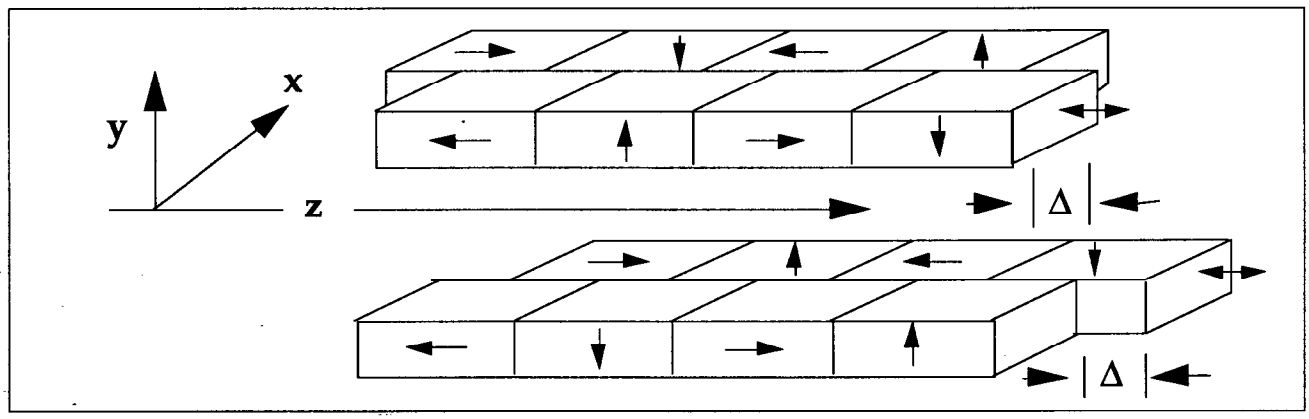

Figure 1: One period of the EPU magnet array with arrows indicating the easy axis of magnetization for each magnet block. All four rows of magnet blocks may be moved longitudinally; moving the two rows with double headed arrows with respect to the other rows changes the helicity. The phase Δ/λ is considered to be at zero when the rows are aligned without overlap.

The EPU has four rows of magnets, all of which may be moved longitudinally by $\pm \lambda/2$. The helicity of the magnetic field and the trajectory, and hence the polarization of the x-rays, is set by moving second and fourth quadrant rows (in the same direction) with respect to the rows in the first and third quadrants. We refer to the polarization setting as 'row phase', to the relative motion of top and bottom arrays as 'jaw phase' and to the relative motion of the second and third quadrant rows with respect to the first and fourth quadrant rows as 'pair phase'. For any value of gap and period length there is a value of row phase which will generate a circular helix; see figure 4. The opposite phase shift will generate a field helix of opposite sense, and hence x-rays of opposite helicity. The design we have adopted calls for a single undulator that will generate x-rays of only one helicity at a time, as opposed to a two-undulator chicane-and-chopper design that would generate both helicities. Our design choice produces more flux, it uses the central path in the monochromator optics and does not require a chopper. Experimentalists will be able to switch helicity by shifting the undulator mechanically. Such switching is slower than a chopped system, but the other advantages were considered valuable.

The magnet design is determined by the electron beam energy, the minimum gap, and the remanent field of the magnet material available. We assume that SPEAR will run at 3 GeV, and that we can use a gap as small as 30 mm. In the past, the most common permanent magnet materials for undulators were SmCo and NdFeB, with the latter preferred for its greater field strength and lower cost. The grades of NdFeB used to date have had a remanent field Br of about 1.1 T, but there are now materials available with Br up to 1.3 T. We chose an NdFeB material from Sumitomo Special Metals called Neomax 35H which has Br = 1.21 T, Hcb = 11.6 kOe, and Hci > 17 kOe.

Analytical expressions for the EPU fields, trajectories, and radiation are complicated, particularly when end effects are considered; we modeled all quantities numerically. We wrote programs based on finite element decomposition of the magnet blocks and assumed contiguous magnet blocks of square cross section and unity permeability. To determine the period length, we assumed magnets with Br = 1.2 T, and then found the magnetic field that will generate x-rays at the minimum energy, E_f = 550 eV. The following relations apply:

$$E_f\ (\text{eV}) \;=\; \frac{950\, E_e^2\ (\text{GeV})}{\lambda\ (\text{cm})\ \left(1 + K^2/2\right)}\ , \qquad K = .934\, B(\text{T})\, \lambda\ (\text{cm})\ , \qquad B = \sqrt{B_x^2 + B_y^2} \tag{1}$$

E_f is the energy of the fundamental, E_e is the electron energy, B is the magnetic field, and λ is the period length of the magnet array.
From these equations, we can generate the plots in Figure 2:

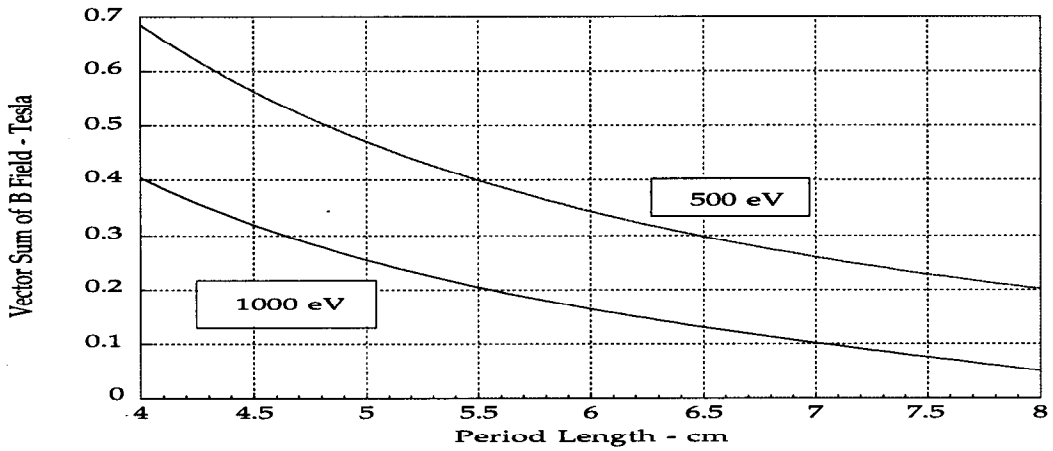

Figure 2: B field as a function of period length, for extreme values of x-ray fundamental energy, based on equations 1.

The lowest E_f is generated at minimum gap, 30 mm. The phase shift and the period length are coupled. We find that a period length of 6.5 cm and a phase shift of 0.168 period will generate Bx = By = 2.02 kG, for a vector sum magnitude of B = 2.86 kG, which lies below the 500 eV curve in Figure 2, at approximately 550 eV. A period length of 6.5 cm will allow 27 periods in 175.5 cm. Additional space is required so that each row can be moved in phase by $\pm \lambda/2 = \pm 3.25$ cm. We also allow some space at the end of each row for field integral corrector magnets. The gap value required to generate 950 eV circularly polarized x-rays is 42.5 mm; the phase value for equal field magnitudes at this gap is 0.146; the field magnitudes are 1.021 kG and the resultant vector sum is 1.444 kG. For any value of the phase that yields equal field magnitudes, the fields are 90^o apart in longitudinal phase.

3. MAGNETIC FIELDS

Figure 3 shows a plot of the first five periods of the longitudinal field profiles:

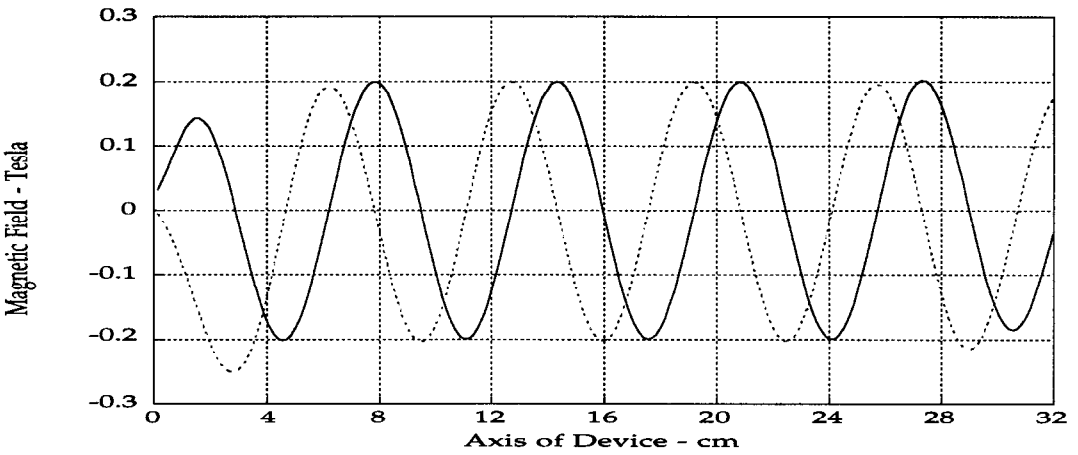

Figure 3: Longitudinal field profiles for the EPU with 6.5 cm period length, 30 mm gap, and a phase shift of 0.168 period (1.092 cm). The dotted curve is the Bx field; the larger first peak will cause a vertical displacement of the trajectory; the solid curve is the By field; its small first peak allows the trajectory to stay on axis in the horizontal.

The phase shift for equal field magnitudes and circular polarization depends on gap, as shown in figure 4:

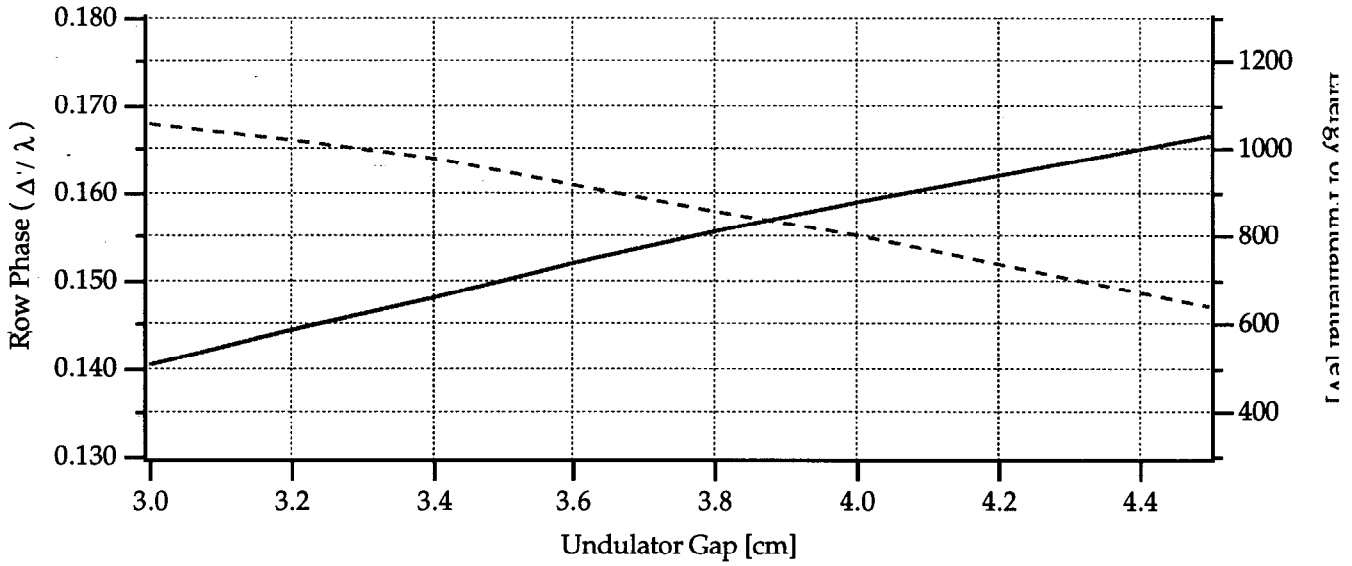

Figure 4: Dependence of EPU phase shift (dashed line) and energy (solid line) of x-ray fundamental upon undulator gap, for 6.5 cm period length.

We have chosen a zero row phase value where the vertical field vanishes and the horizontal field remains. This choice of zero results in short travel between the right and left circularly polarizing field configurations, and will itself yield x-rays polarized in the vertical plane. At zero phase and minimum gap, the field strength has a maximum value of 2.35 kG, for an x-ray fundamental energy of 652 eV. At a row phase value of ± 1/2 period, the horizontal field vanishes and the vertical field remains. This condition will yield x-rays polarized in the horizontal plane. At minimum gap, the field strength has a maximum value of 4.04 kG, for an x-ray fundamental energy of 328 eV.

Having established the period length, we investigated the transverse horizontal and vertical field profiles. The peak magnetic field strength profiles were calculated for the phase which generated circular polarization, and minimum gap. Figures 5 and 6 show the results.

The small width of the horizontal magnetic field peak implies that if the electron beam is mis-steered horizontally, the resulting x-rays will not be polarized as expected, and their energy will be blueshifted. In fact, if the phase is set correctly for circular polarization, the blue shift may be used as an indicator of the degree of ellipticity of polarization. However, there will be a locus of x,y coordinates for which the blueshift caused by horizontal errors will be offset by the redshift caused by vertical displacement.

To correct a horizontal error, there are four strategies: 1) If the error is parallel to the correct axis, it is possible on beamline 5 to move the undulator horizontally. 2) The trim coils and SPEAR electron optics may be used with SPEAR BPM's to steer the beam down the axis of the undulator. Such a strategy would be particularly effective for horizontal angular error correction. 3) The phase of the device may be shifted, so as to undo the ellipticity caused by the off-axis beam. 4) Users can measure the ellipticity of the beam and normalize their data to include this effect; they will need some means of monitoring the ellipticity in any case.

Co-Pd multilayers have been used to determine relative ellipticity.[7] The strength of the magnetic circular dichroism effect was observed in two samples, which were magnetized in opposite directions. The accuracy of this determination was about 5%. Such an experiment can apparently be used to determine the minimum value of ellipticity as undulator or electron beam position was varied.

We modeled the EPU with various transverse gap values to see whether a gap between the rows in each jaw could be used to flatten the horizontal field. The main effect is a deep notch in the vertical field. It would take a transverse gap of 1 cm to achieve appreciable flattening of the horizontal field, and this causes a 50% notch in the vertical field profile. This study also showed the minimal effect of the 1 mm gap we will leave between the rows.

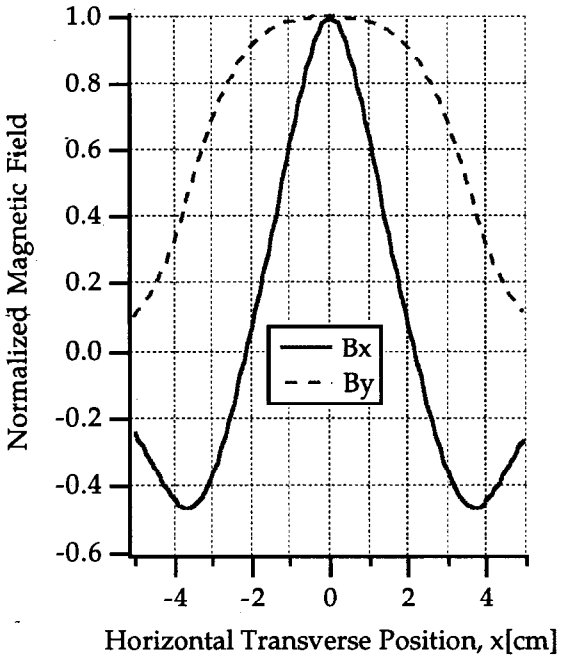

Figure 5: Transverse horizontal field profiles for a magnet row width of 40 mm, and with the rows touching each other. The peak field values are shown, with the phase =168 period, period length = 6.5 cm, and gap = 30

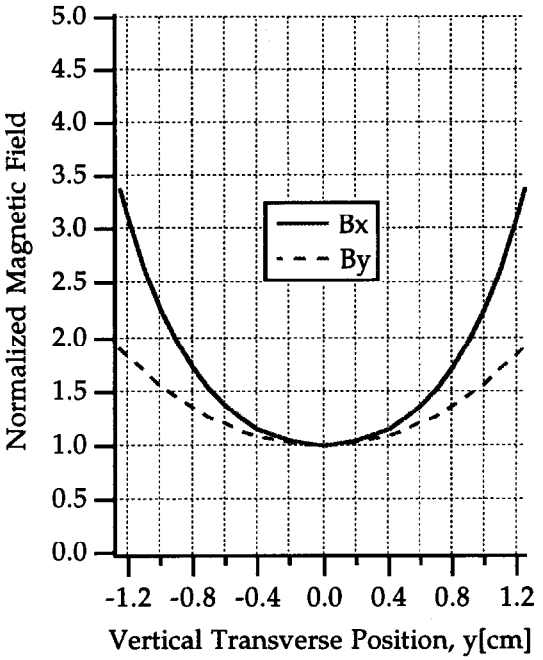

Figure 6: Transverse vertical field profiles for a magnet row width of 40 mm, and with the rows touching each other. The peak field values are shown, with the phase = .165 period, period length = 6.5 cm, and gap = 30 mm.

4. PHASE CHANGE EFFECTS

We constructed earlier a linearly polarizing undulator based on the principle that its magnetic field could be varied by changing the phase between its upper and lower jaws.[8] This adjustable phase undulator (APU) was a standard one-row-per-jaw Halbach device in construction, but we could vary the energy of the x-ray output by moving one row with respect to the other one, without changing the gap. It offers several advantages. It is much less elaborate to build than an adjustable gap device and its vertical field integral is unchanged when the phase is changed, so it needs negligible changes of dipole correction compared to an adjustable gap device. Also, its vertical focusing strength is constant in phase, so it does not change the tune of the ring as it would if the gap were changed.

We wanted to apply the APU principle to the elliptically polarizing case, and we found that there are two ways of doing this. Having set the polarization with row phase, we can then tune the net strength of the magnetic field by changing the jaw phase, or by changing the pair phase. Changing the jaw or pair phase requires small adjustments of row phase to keep the rate of elliptical polarization constant. The EPU could be built without gap adjustability, since polarization and energy could be varied by changing only phases. This concept combines the Sasaki design and the APU design; with the combination we have vertical and horizontal linear polarization, and both senses of circular polarization, all variable in energy by changing phases.

Figure 7 shows the variation in transverse magnetic field strength with jaw phase and pair phase for circular polarization, and for vertical and horizontal linear polarization. This aspect of the EPU design will be more fully described in another article. [9]

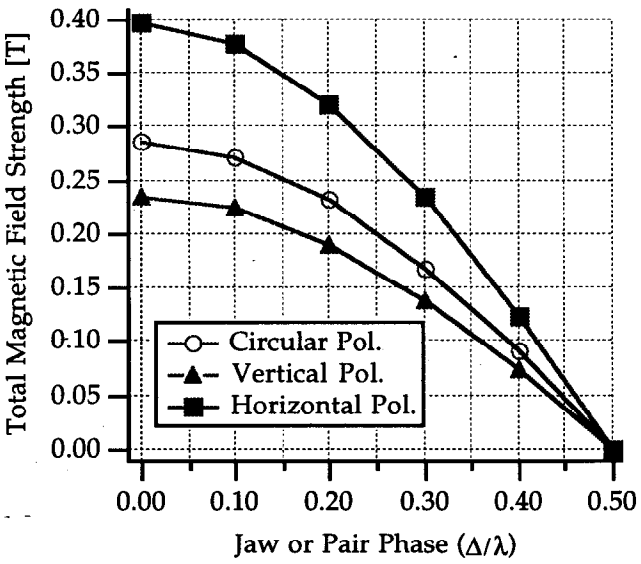

Figure 7: Variation of transverse magnetic field, $\sqrt{(B_x^2 + B_y^2)}$, with jaw and pair phase, for circular, vertical, and horizontal polarization modes.

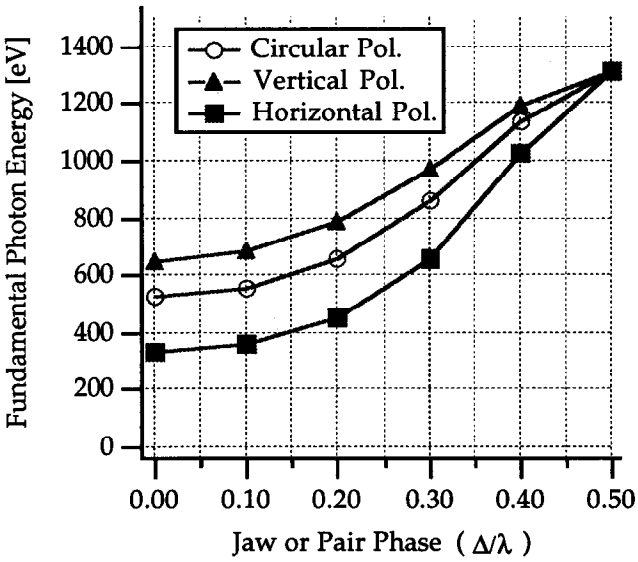

Figure 8: Variation of energy of the peak of the fundamental, with jaw and pair phase, for circular, vertical, and horizontal polarization modes.

5. ELECTRON TRAJECTORIES

The trajectories of electrons in the EPU depend on how the end termination of the magnetic blocks is done. If the usual half blocks are used at each end, the trajectory is displaced in the vertical, but not in the horizontal, as shown in figure 9. This is contrary to what happens in a plane polarizing undulator where the trajectory is displaced horizontally; for all values of the row phase, there is no deflection of the horizontal trajectory. If we wish to have minimal displacement in x and y, we might

use the 1/4, 1/2, and 3/4 block end termination scheme of Halbach.[10]

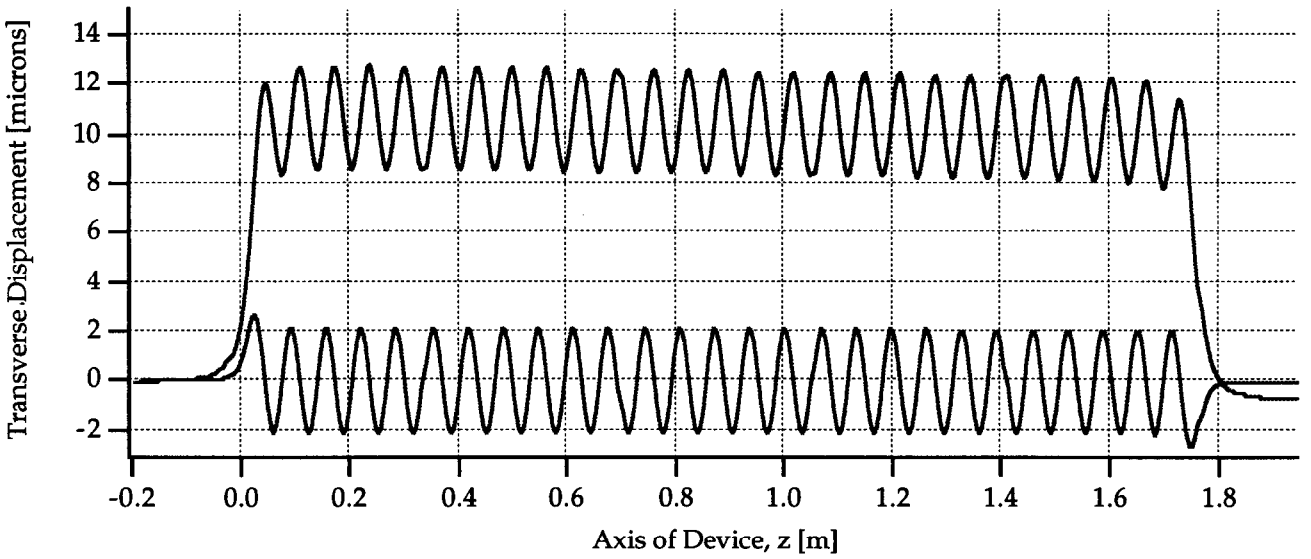

Figure 9: EPU electron trajectories in the vertical (upper curve) and horizontal (lower curve) directions. The relative phase between the trajectories is 90^{o}.

The trajectories of electrons were calculated using a fourth order Runge-Kutta solution of the Lorentz force equations. The on-axis trajectories for the minimum gap circular polarization case are shown in Figure 10. Figure 11 shows the trajectories of electrons which are off-axis by one half the 3σ horizontal width of the electron beam.

In figure 10, the trajectory is circular, except for the entrance and exit paths. In figure 11, the trajectory is elliptical, so the radiation is elliptically polarized. Also, the trajectory center slips sideways, which will deflect the axis of the radiation cone. The smaller horizontal diameter of the ellipse in figure 11 than the circle in figure 10 indicates a blueshift of the energy of the radiation.

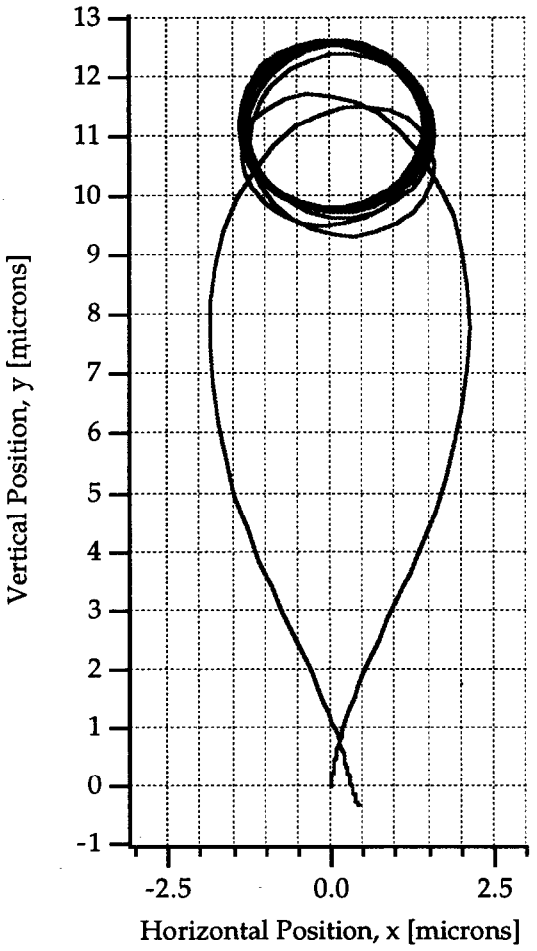

Figure 10. End view projection of the electron beam trajectory onto the transverse plane. This trajectory was calculated for gap = 30 mm, jaw phase = 0.27, row phase = 0.168, and on-axis injection of 3 GeV electrons.

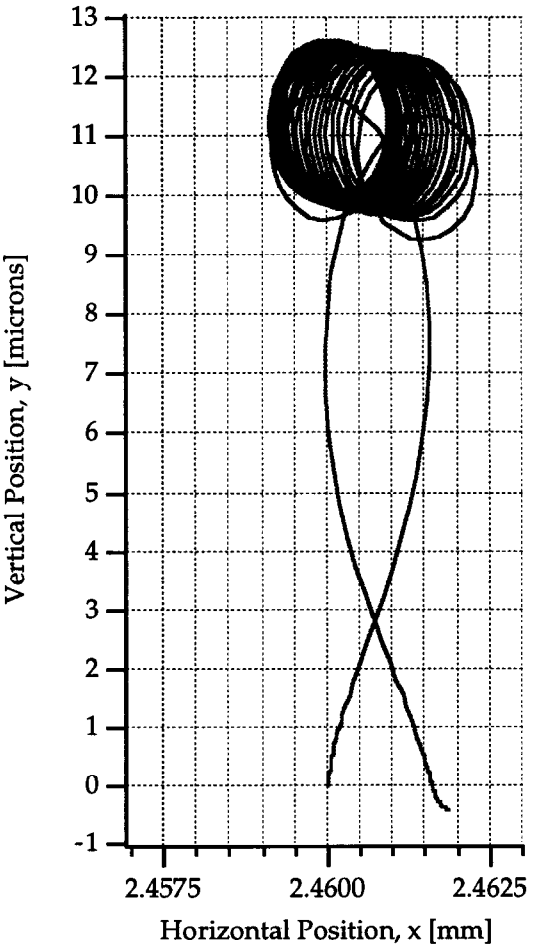

Figure 11: End view projection of the electron beam trajectory onto the transverse plane. This trajectory was calculated for gap = 30 mm, jaw phase = 0.27, row phase = 0.168, and for 3 GeV electrons displaced horizontally by 2.46 mm from the axis.

6. RADIATION AND POLARIZATION

Figure 12 shows the fundamental peak of the x-ray spectrum at 800 eV, calculated for the case of an emittance broadened electron beam with on-axis trajectory. For the EPU, we need to calculate both the effects of emittance on the undulator spectrum, and on the polarization rate. We considered acceptance of the entire central cone in the far field. These curves were calculated by a new radiation code developed by S.L. and are based on the direct integration of standard radiation formulae[11] over the electron beam trajectory, with emittance included via convolution with a gaussian distribution of electron beam angular divergence.[12] Polarization rates are defined as the normalized Stokes' vector components, and degree of polarization as their sum in quadrature.[13]

Figure 12 shows that the EPU is capable of producing highly polarized radiation over the entire useful portion of the fundamental peak. The degree of circular polarization is close to unity at the peak, while the degree of linear polarization is near zero. The skew-linear polarization rate (i.e.. the degree to which the electric field vector of the radiation is polarized at an angle of 45 or 135 degrees to the x-axis), is nearly zero across the entire fundamental peak.

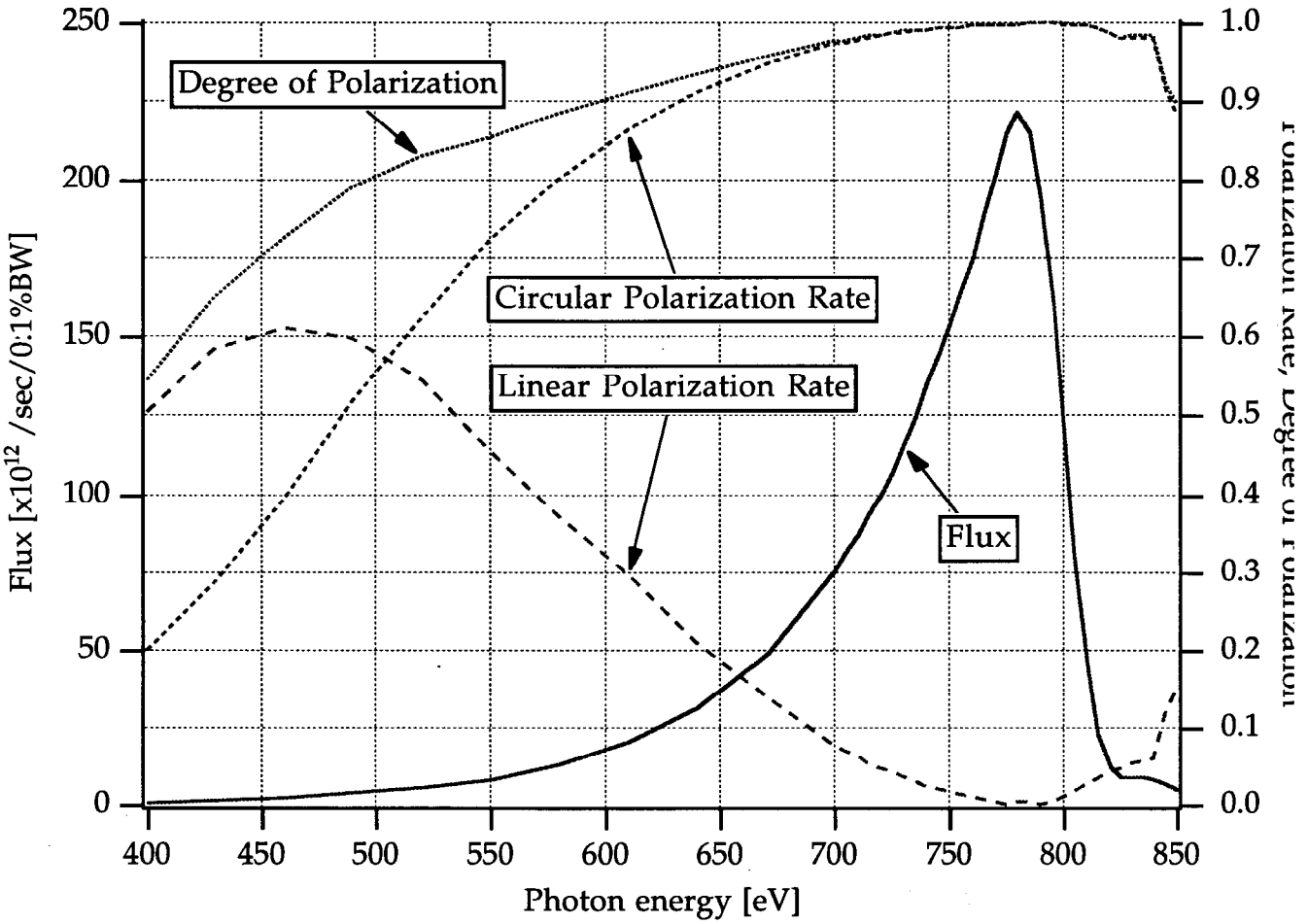

Figure 12: Integrated flux and polarization characteristics of the first harmonic of the EPU in circular polarization mode. The EPU parameters used were: gap = 30mm; jaw phase = 0.27; row phase = 0.168, E_f = 800 eV The electron beam parameters are defined above, and on-axis injection was assumed. The same curves would be obtained if the jaw phase were zero and the gap were set for 800 eV.

The emittance of SPEAR is large, and it causes considerable broadening of the spectra of the existing beamline 5 linearly polarizing undulators. An undulator should have a fundamental peak of width $\Delta E/E = 1/N$ where N is the number of periods. The existing 30 period undulator, for example, should have a peak width of 30 eV FWHM at E_f = 900 eV, but emittance broadens this to about 80 eV. This is comparable to the broadening calculated in figure 12 for the EPU.

A circularly polarizing undulator creates only first harmonic radiation on axis. This frees the magnet designer somewhat, because the errors that harm useful higher harmonics in linearly polarizing devices do not need to be considered. Figure 13 shows the additional harmonic content of the radiation field as it is observed over the entire central cone and averaging over the emittance was included. The total flux envelope in the fundamental peak is shown, as well as the individual contributions to the total flux from electrons travelling parallel to the optic axis and at an angle corresponding to 1.5 $\sigma_{x'}$ in the horizontal plane.

The power emitted at different values of row phase varies as $B_x^2 + B_y^2$; for given value of gap, there is more power emitted at larger values of row phase; the minimum occurs for the vertically polarizing condition. This will cause the heat load on optical components to vary when the phase is switched.

On-axis electrons contribute the bluest portions of the fundamental peak, and their radiation is all circularly polarized. The off-axis electrons have their contributions red-shifted in accordance with their angular deflection. Also, when viewing these electrons, one is no longer looking directly down the center of a helix, but off to one side of the helix, and the longitudinal

source size now becomes apparent. The radiation field is now no longer purely circular, but is elliptical, and as such can be decomposed into circularly polarized and linearly polarized components. The linearly polarized radiation will have a spectrum composed of a fundamental harmonic as well as higher harmonics. The harmonic content of the off-axis electrons is also shown in Figure 13. While the fundamental harmonic contains the most useful flux, the 2nd, 3rd, and 4th harmonics will also be present in slight amounts. This is an emittance effect; a machine with smaller emittance will show less harmonic structure.

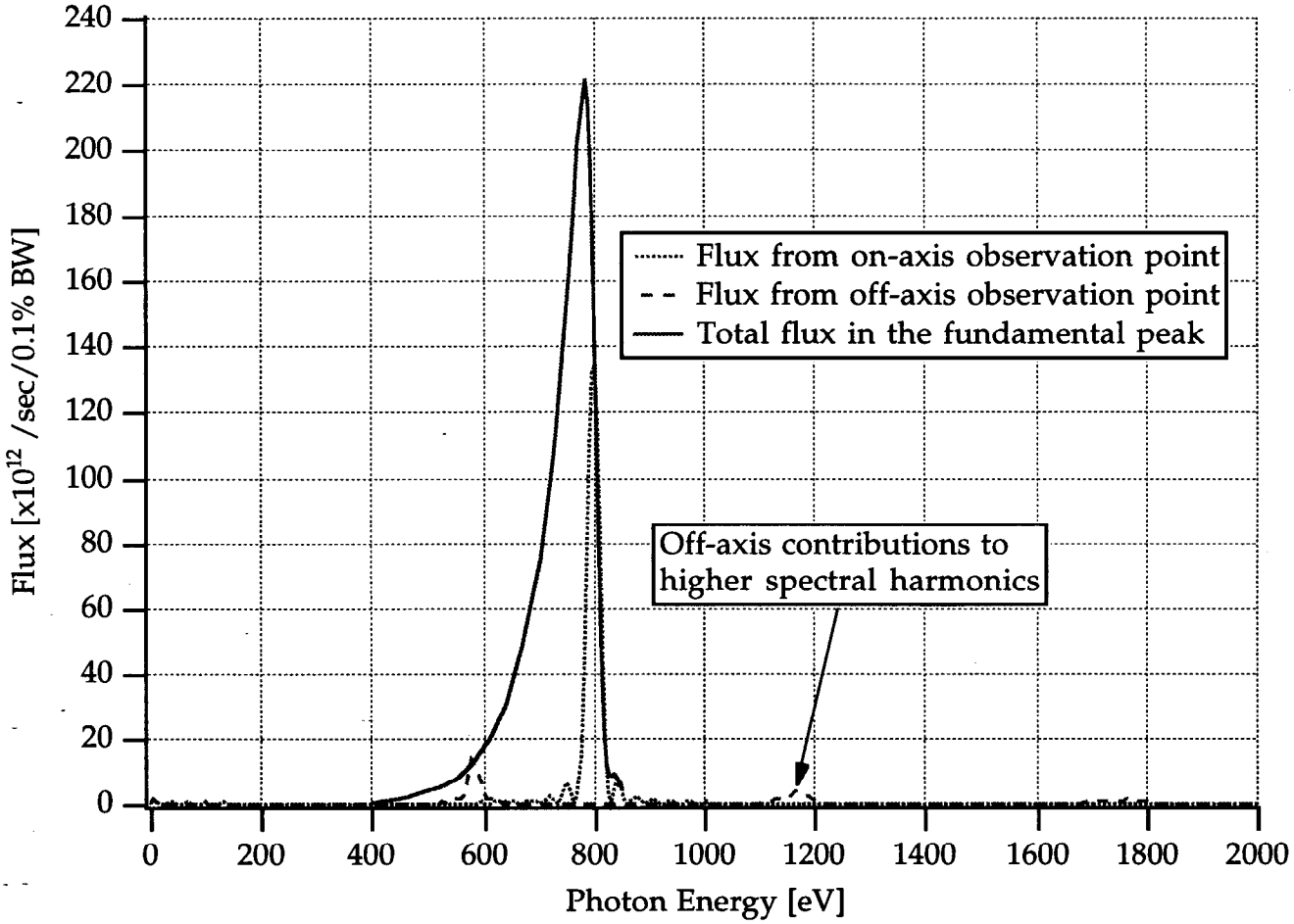

Figure 13: Harmonic content of EPU under circular polarization mode. Undulator parameters used were: gap = 30mm; jaw phase = 0.27; row phase = 0.168.

7. MECHANICAL AND MAGNETIC DESIGN CONSIDERATIONS

To build the EPU, we have only to construct two magnet assemblies, which we will mount in the existing beamline 5 undulator mover. The mechanical design is different from an ordinary one-row-per-jaw undulator because of the proximity of the rows comprising each jaw. We could not constrain the magnets mechanically on three sides, so we will glue them to the keeper using only the lower surface. The blocks will be coated with vacuum deposited aluminum, which is then chromate passivated. We plan to use a fast-curing radiation-resistant Loctite Corp. N^{o} 325 adhesive. We acquired from the Field Effects division of Intermagnetics General Corp. a clever technology for additional constraint for the magnets; the rows will

be 'shrink-wrapped' in thin non-magnetic metal foil; this acts as insurance against a failure of the adhesive or breakage of the blocks.

There are considerable forces, which vary sinusoidally with relative phase, between jaws, and between rows within a jaw; the inter-row forces are greater. Figure 14 is an end view of one jaw assembly, showing crossed roller slides between backing beams on which the magnet keepers are mounted; these slides resist the horizontal forces. There are three pairs of inter-row bearings; one is in the longitudinal center of the beams to resist horizontal beam flexing. The crossed roller slide units on the outboard sides support the beams vertically; there are two sets of these bearing units, which connect the beams to two fixtures. The fixtures are attached to horizontal cross members of the existing undulator mover at the Airy points of the beams. The bottom plate of the fixture will hold electromechanical actuators and encoders, which attach to the centers of the beams.

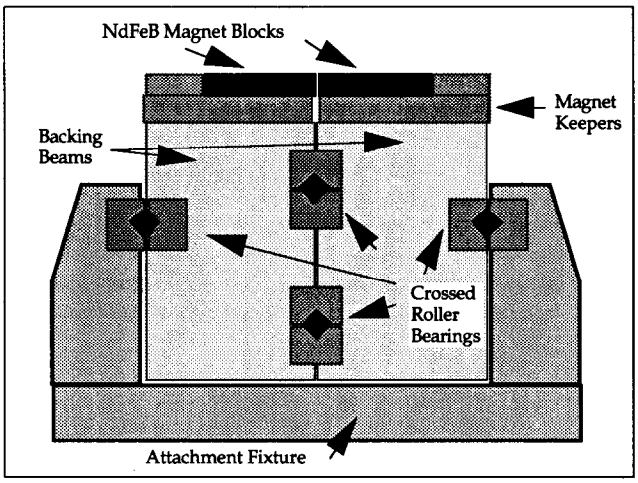

Figure 14: End view of one of the magnet jaw assemblies. The large rectangles are cross sections of rigid beams which support all the magnet keepers. The magnet blocks are held onto the keepers by an adhesive and there is a thin foil cover over the magnets and keepers. The middle two crossed roller bearings hold the two backing beams together and in alignment; the outside pair attach the beams to a fixture, which is fixed to the undulator mover.

The errors from the mean value of Br of each magnet block will be measured in the three principle directions, and these errors will be fed to a simulated annealing algorithm to sort the magnets in order to minimize the effects of the errors. [14] The magnets were specified to have deviations from
 of no more than 1.5% and angular deviations from the easy axis of no more than 1.5^{o}. At the very least, we will minimize the least squares differences between the measured magnetic field and an ideal sinusoidal field when the blocks are arranged in four separate rows. For the EPU, minimizing errors between vertically opposed magnets could only be done at one phase anyway. We will also calculate trajectories from the annealed magnet arrays to make sure that the sorting leaves errors no larger than will be hidden by SPEAR's emittance. This procedure may not be very helpful in the EPU case, because the effective fields are those at the ends of the magnets, near the gap between rows.

We plan to place the EPU in a jig where the magnet jaws will be horizontally opposed, and put this assembly on a precise coordinate measuring machine (CMM) at SLAC. After the assembly is aligned mechanically, we will place a Hall effect sensor on the probe arm of the CMM and sweep the gap to measure the magnetic fields. Since there are fields in all directions, we expect Hall probe measurements to be complicated by the tensor response of the Hall probe; we may prefer measurements with short integrating coils. We expect to measure dipole, quadrupole, sextupole, and possibly octupole fields and their integrated values. We will then install arrays of small magnets which can be moved in the 'y' direction at the ends of each row. This 'magic fingers' technique is described by Hoyer.[15] By adjusting these small blocks of permanent magnet material, we hope to null the field integral errors near the axis at at least one value of gap. If we operate the EPU in phase adjust mode only, we expect that the settings of these small magnets will be invariant. We hope this technique may allow us to move the EPU between right and left circularly polarizing modes with negligible effects on the electron beam.

8. SUMMARY

We have presented the design for a new type of planar helical undulator to produce circularly polarized photons in the 550 - 950 eV range. The design allows for tuning both the x-ray energy and the polarization state of the radiation by sliding the four rows of the undulator longitudinally, at constant gap. We presented calculations of the magnetic fields, electron beam trajectories, radiation fields and polarization rates, taking emittance into account.

The EPU will produce radiation that is linearly polarized in the vertical or the horizontal, or elliptically polarized in the left or right handed sense. The ability to obtain vertically polarized radiation could be exploited in higher energy storage rings for diffraction experiments; it would allow the experimenter to have a goniometer with a vertical axis so that samples could be placed with their surfaces horizontal.

The EPU design also could be executed with no gap adjustability, which would considerably simplify the construction and operation of the undulator. We expect that a pure adjustable phase EPU would not change its dipole steering strength as its phase was varied, as in the APU case. We also expect that its focusing strength would not vary in the horizontal or the vertical as its phase was changed, as with the APU . These are three possible advantages of a phase adjustable EPU over a gap adjustable EPU. Because we are mounting the EPU on a gap adjustable mover, and because we can move all four rows of magnets, we will be able to test both principles.

9. ACKNOWLEDGEMENTS

Several people made welcome and valuable contributions to this work. Roland Savoy, now at Siemens, Helmut Wiedemann of SSRL, Klaus Halbach of LBL, and Shigemi Sasaki of JAERI contributed useful technical comments. Brian Kincaid and Kwang-Je Kim of LBL supplied generous technical and material support for S.L. to perform the numerical modeling for the EPU. Mr. Takeo Takada of Shin-Etsu Chemical Co. provided excellent support by analyzing the undulator with several additional calculations. Mr. Kane Zuo of SSRL was responsible for the mechanical design. The authors thank all of these people for their friendly help. R.C. is supported by the U. S. Department of Energy, Office of Basic Energy Sciences, Division of Materials Science. S.L. was supported by the Director, Office of Energy Research, Division of Basic Energy Sciences, of the U.S. Department of Energy under Contract Number DE-AC03-78SF00098.

10. REFERENCES

1 S. Sasaki, K. Miyata, and T. Takada, Jpn. J. Appl. Phys. 31 (1992) p. L1794.

2 K. Kakuno and S. Sasaki, 'Conceptual Design of Vertical Undulator', JAERI-M Report 92-157 (1992).

3 R. Carr, Proceedings of the 1993 IEEE Particle Accelerator Conference.

4 R.Z. Bachrach, R.D. Bringans, B.B. Pate and R.G. Carr, SPIE Proceedings 582 (1985) p. 251.

5 H-D. Nuhn, SSRL ACD Note #118 revised May, 1992.

6 K. Halbach, Nucl. Inst. & Methods 187 (1981) p. 109.

7 L.J. Terminello, G. D. Waddill, & J.G. Tobin, Nucl. Inst.& Methods A319 (1992) p. 271.

8 R. Carr, Nucl. Inst. & Methods A306 (1991) p. 391.

9 S. Lidia and R. Carr, Proceedings of the 1993 Synchrotron Radiation Instrumentation Conference, Gaithersburg Md.

10 K. Halbach, Nucl. Inst. & Methods A250 (1986) p. 95.

11 C. Wang and Y. Xiao, "On Algorithms For Undulator Radiation Calculation," in the Proceedings of the International Conference on Synchrotron Radiation Sources, Indore, India, 1992, S.S. Ramamurthi, G. Singh, and D. Angal, eds.

12 See, for example, K.-J. Kim, "Characteristics of Synchrotron Radiation," in AIP Conference Proceedings 184, Physics of Particle Accelerators, Vol. 1, M. Month and M. Dienes, eds. American Institute of Physics, New York, 1989.

13 See, for example, M. Born and E. Wolf, Principles of Optics , Pergamon Press, 1987 , p. 555.

14 A.D. Cox and B.P. Youngman SPIE Proceedings 582 (1985) p. 91.

15 E. Hoyer, LBL Engineering Note N^{o} M7354, May, 1993.